Lab on a Chip

Accepted Manuscript

This is an *Accepted Manuscript*, which has been through the Royal Society of Chemistry peer review process and has been accepted for publication.

Accepted Manuscripts are published online shortly after acceptance, before technical editing, formatting and proof reading. Using this free service, authors can make their results available to the community, in citable form, before we publish the edited article. We will replace this *Accepted Manuscript* with the edited and formatted *Advance Article* as soon as it is available.

You can find more information about *Accepted Manuscripts* in the **Information for Authors**.

ROYAL SOCIETY OF CHEMISTRY

www.rsc.org/loc

Graphical Abstract

A simple, high-efficiency, clamshell-style, superhydrophobic plasma separator for point-of-care applications.
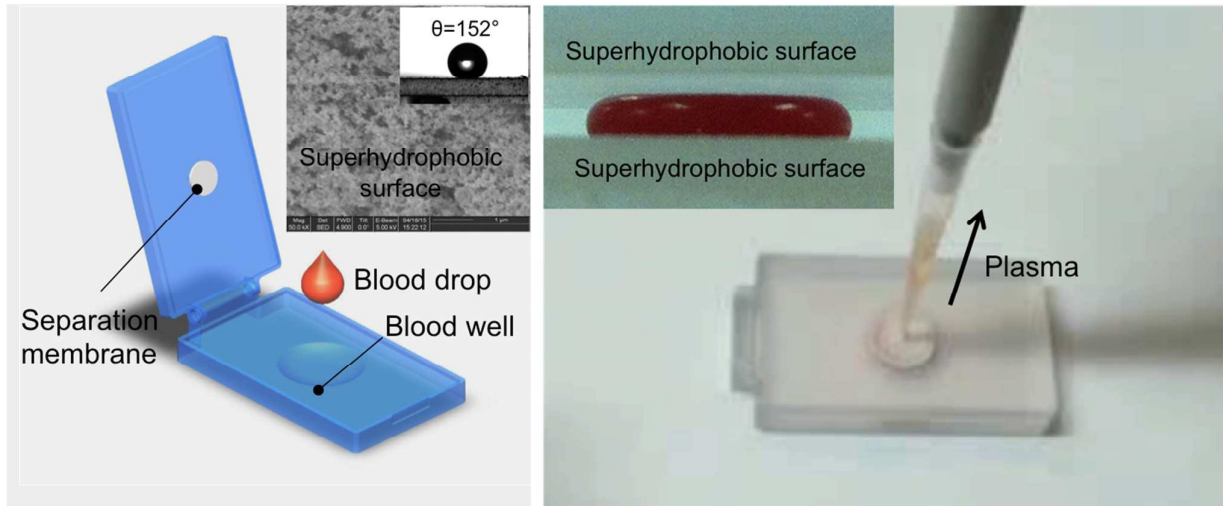
A High-Efficiency Superhydrophobic Plasma Separator

Changchun Liu[1*], Shih-Chuan Liao[1,5], Jinzhao Song[1], Michael G. Mauk[1], Xuanwen Li[2], Gaoxiang Wu[3], Dengteng Ge[3], Robert M. Greenberg[4], Shu Yang[3] and Haim H. Bau[1]

[1]Department of Mechanical Engineering and Applied Mechanics,

[2]Institute for Translational Medicine and Therapeutics, Perelman School of Medicine

[3]Department of Materials Science and Engineering, 3231 Walnut Street, Philadelphia, PA 19104, USA

[4]Department of Pathobiology, School of Veterinary Medicine

University of Pennsylvania, Philadelphia, Pennsylvania 19104, USA

[5]Department of Biomechatronics Engineering, National Pingtung University of Science and Technology, Pingtung 912, Taiwan, ROC

[*] **Corresponding author**

Dr. Changchun Liu

Department of Mechanical Engineering and Applied Mechanics

University of Pennsylvania

210 Towne Building

220 South 33rd St.

Philadelphia, Pennsylvania 19104-6315, USA

Phone: (215)898-1380

E-mail: lchangc@seas.upenn.edu

1

Abstract

To meet stringent limit-of-detection specifications for low abundance target molecules, a relatively large volume of plasma is needed for many blood-based clinical diagnostics. Conventional centrifugation methods for plasma separation are not suitable for on-site testing or bedside diagnostics. Here, we report a simple, yet high-efficiency, clamshell-style, superhydrophobic plasma separator that is capable of separating a relatively large volume of plasma from several hundred microliters of whole blood (finger-prick blood volume). The plasma separator consists of a superhydrophobic top cover with a separation membrane and a superhydrophobic bottom substrate. Unlike previously reported membrane-based plasma separators, the separation membrane in our device is positioned at the top of the sandwiched whole blood film to increase the membrane separation capacity and plasma yield. In addition, the device's superhydrophobic characteristics (i) facilitates the formation of well-defined, contracted, thin blood film with a high contact angle; (ii) minimizes biomolecular adhesion to surfaces; (iii) increases blood clotting time; and (iv) reduces blood cell hemolysis. The device demonstrated a "blood in-plasma out" capability, consistently extracting 65 ± 21.5 µL of plasma from 200 µL of whole blood in less than 10 min without electrical power. The device was used to separate plasma from *Schistosoma mansoni* genomic DNA-spiked whole blood with a recovery efficiency of $> 84.5 \pm 25.8$ %. The *S. mansoni* genomic DNA in the separated plasma was successfully tested on our custom-made microfluidic chip by using loop mediated isothermal amplification (LAMP) method.

2

Introduction

Plasma extraction or separation from raw whole blood is usually required for blood-based clinical diagnostics because i) the inclusion of blood cells or components such as hemoglobin may inhibit subsequent DNA or RNA polymerases in enzymatic amplification tests (e.g., PCR), leading to an unreliable quantification or even false negatives;[1] ii) inhibitors from whole blood can also interfere with immunoassays and result in low sensitivity;[2] and iii) many accepted standards of care are based on pathogen levels in cell-free plasma rather than whole blood.[3-6] For example, HIV viral load testing is based on detecting cell-free virus in blood, but not reverse-transcribed viral DNA integrated in the chromosomes of blood cells. Centrifugation is one the most widely used methods for plasma separation in biomedical laboratories. However, centrifugation is not suitable for on-site or bedside applications. Centrifuges may also not be available in sufficient numbers even at hospitals in resource-constrained settings. Hence, it is desirable to develop simple inexpensive plasma separation methods that can operate without electricity.

In the past decade, different approaches have been reported to extract plasma from whole blood at the point of care,[7] including capillary imbibition,[8] blood cell sedimentation,[9,10] and cross-flow filtration.[11,12] However, these methods either require a pre-dilution prior to blood separation or operation with minute volumes of blood (<10 µL). Extensive dilution may, however, adversely affect the limit-of-detection, which is critical in many clinical samples with relatively low abundance target molecules. Minute volumes of plasma cannot provide sufficient target for amplification such as needed for the monitoring of HIV viral load,[13-15] and the detection of cell-free nucleic acids (cfNAs).[16-20] For example, the state of the art limit of detection of HIV viral load is 50 copies/mL. At this concentration, most 1 µL blood samples will contain no virus at all. Even if one is content with a limit of detection of 1000 copies/mL (a concentration of HIV virus that requires change of therapy),[21] many 1 µL blood samples will present negative. To address this need, several membrane-based plasma separators have been developed and tested for extracting a relatively large volume of plasma.[22-25] Homsy *et al.*[22] described a bottom-positioned, membrane-based, blood filtration element (BFE), capable of extracting 12 µL of plasma from 100 µL of undiluted whole blood. The device used an external vacuum pump to provide a negative pressure for plasma extraction. Wang *et al.*[23] reported a microfluidic chip with an embedded 2 µm pore size bottom-positioned membrane filter to

3

separate plasma and HIV virus. However, all these bottom-positioned membrane configurations are susceptible to clogging, leading to a low separation capacity and low plasma yield. To address this shortcoming, our group has previously developed a vertically-positioned membrane-based, sedimentation-assisted, plasma separator, which is capable of extracting 275 µL of plasma from 1.8 mL of undiluted whole blood.[26] However, this device requires collecting more than milliliters of venipuncture blood, which is relatively invasive and incompatible with onsite testing. In particular, children below 24 months of age are restricted to 700 µL of whole blood draws.[27] In comparison, finger or heel-prick blood sampling is less invasive and more convenient than venipuncture sampling,[28-30] and has been validated against standard phlebotomy in clinical testing.[31] There is a clear need for a high-efficiency, rapid, non-instrumented, point-of-care (POC) plasma separator for extracting a relative large volume of plasma from several hundred microliters of finger or heel-prick blood (maximum volume is 250-500 µL[32,33]), instead of milliliters of venipuncture blood sampling.

Superhydrophobic surfaces, as seen in lotus leaves, typically have a water contact angle greater than 150 ° and a small roll-off angle (< 10°). These surfaces are self-cleaning, that is, water droplets can roll off these surfaces at a very small tilt angle and carry away dust particles and debris.[34,35] Superhydrophobic coatings have been applied to surfaces to repel bioparticles due to their excellent anti-adhesion and anti-biofouling properties.[36,37] In recent years, there has been an increasing interest in incorporating superhydrophobic surfaces into microfluidic devices for fluid manipulation[38,39] and bioanalytical applications.[40,41]

Here we report a new, simple, inexpensive, disposable, high-efficiency, clamshell-style, superhydrophobic plasma separator for relatively large-volume plasma extraction from several hundred microliters of whole blood. Unlike previously reported membrane-based separators,[22-26] our superhydrophobic separator takes advantage of: i) the combination of gravitational sedimentation of blood cells and a top-positioned membrane filtration mechanisms to reduce membrane clogging and to enable the extraction of relatively large plasma volume, and ii) superhydrophobic characteristics to reduce the loss of target biomolecules and to prevent the sandwiched blood film from spreading. We demonstrated an extraction of 65 ±21.5 µL of plasma from 200 µL of whole blood on our device within less than 10 minutes. The utility of this superhydrophobic plasma separator for molecular diagnostics application was demonstrated by separating plasma from *Schistosoma mansoni* DNA-spiked whole blood. The *S. mansoni* DNA in extracted plasma was tested with our

4

microfluidic chip [26] that carried out nucleic acid isolation and amplification, demonstrating that the plasma was of sufficient purity for polymerase activity. The plasma separator described herein can be used as a stand-alone module to separate the plasma from the whole blood. Accordingly, the device is suitable for onsite testing at home, in the clinic, at bedside, as well as in resource-poor regions of the world, where funds, trained personnel, and laboratory facilities are in short supply, and in settings lacking electrical power.

Experimental

Superhydrophobic plasma separator

The clamshell-style, superhydrophobic plasma separator depicted in **Fig. 1** is 5.4 cm long × 3.0 cm wide × 0.8 cm thick. Both top and bottom substrates were fabricated by 3D-printing (Projet 6000HD, 3D Systems, USA), and hinged together with a pivot joint (**Fig. S1** in Supporting Information). The bottom substrate contains a 13 mm diameter × 1.3 mm deep blood well and is designed to accommodate ~ 200 μL of blood. The top cover has 11 mm diameter × 0.5 mm deep depression. An array of cylindrical micropillars, each 300 μm tall and 500 μm in diameter, was printed into the floor of the depression (inset in **Fig. 1B** and **Fig. S2** in Supporting Information). The micropillar array serves as a support for the plasma separation membrane (Vivid^{TM}, Pall Life Sciences, East Hills, NY). The micropillar array cavity connects to a 1.5 mm diameter vertical via (plasma exit port) (inset in **Fig. 1B** and **Fig. S2** in Supporting Information). The size of the exit port matches tightly the outer diameter of a 200 μL pipette tip that was used to collect the plasma. We applied commercially available, spray-on "Neverwet^{TM}" to form thin superhydrophobic coatings on both substrates in the two-step process suggested by the manufacturer.[42]

The 11 mm diameter, separation membrane was cut by a CO_2 laser cutter (Universal Laser Systems). A double-sided adhesive tape (McMaster-Carr, New Brunswick, NJ) was cut with the laser to the same external dimensions as the membrane. An 8 mm diameter circle (an area of ~ 0.5 cm^2) was removed from the adhesive tape center to leave an annular frame. The adhesive frame was attached to the plasma separation membrane. The resulting laminate was placed on the top of the micropillar array and pasted to the frame surrounding the array to entirely cover the micropillar array.
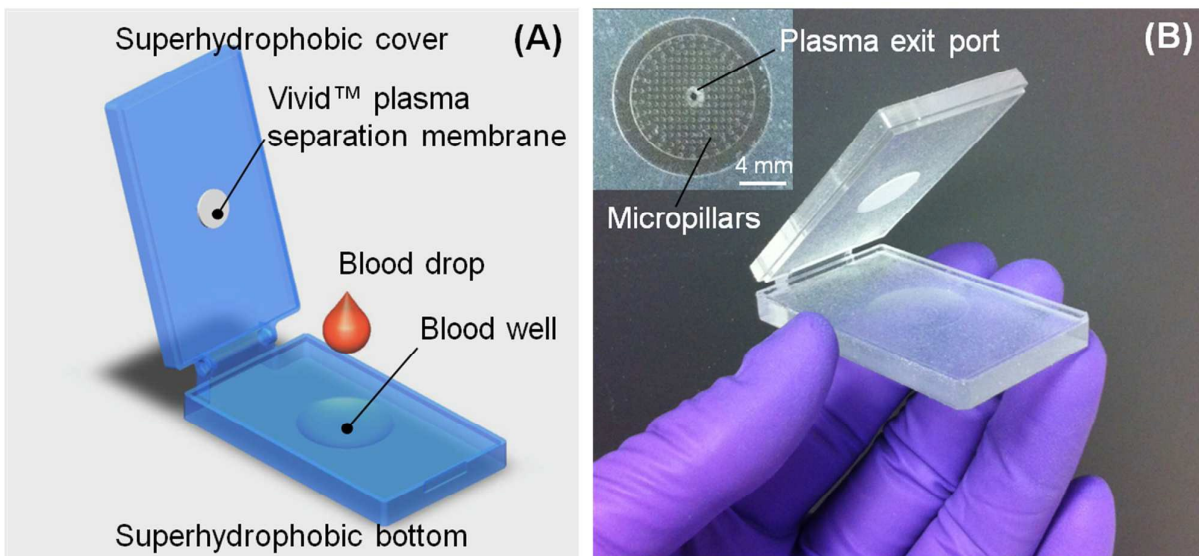
5

Fig. 1: (A) A schematic illustration of a clamshell-style, superhydrophobic plasma separator. The device consists of a superhydrophobic, cover with a separation membrane and a superhydrophobic bottom with a blood well. (B) A photograph of the superhydrophobic plasma separator. Inset is an optical image of a micropillar array located in the depression of the superhydrophobic top cover.

Blood compatibility characterization of spray-on superhydrophobic surface

The morphologies of the spray-on superhydrophobic surface and non-coated 3D-printed substrate were imaged with a scanning electron microscope (SEM) equipped with a focused ion-beam (FIB) (FEI Strata DB235).

To determine whether the superhydrophobic surfaces can reduce biomolecular adhesion, we sandwiched 100 μL of plasma sample spiked with a known *S. mansoni* DNA concentration (50 fg) between the two spray-on superhydrophobic substrates. After 10 min, the plasma was recovered, and the *S. mansoni* DNA in the plasma was detected by real time quantitative loop-mediated isothermal amplification (LAMP). To test the anticoagulant property of the spray-on superhydrophobic coating, 30 μL of fresh blood was dropped onto the surface, followed by incubation at 37 °C for 20 min. Then, the blood was rinsed by DI water. To assess the hemocompatibility of the coating, 200 μL of whole blood was placed on the coated substrate. After 20 min, 4 mL of isotonic saline was added to the blood sample to stop hemolysis. Positive and negative controls were, respectively, produced by adding 200 μL of whole blood to 4 mL of distilled water and to isotonic saline. All the test samples were centrifuged. Optical density (OD) of the supernatant was measured at 540 nm using a ND-1000

spectrophotometer (NanoDrop Technologies, Wilmington, DE).

Sample preparation and device testing

De-identified, EDTA anticoagulated, whole blood samples from healthy donors were collected by the Hospital of the University of Pennsylvania with the approval of the Institutional Review Board (protocol: 814752). All blood samples were handled without any dilution.

200 µL of the whole blood spiked with *S. mansoni* DNA (obtained from the Schistosomiasis Resource Center, for distribution by BEI Resources, NIAID, NIH) was loaded into the blood well (**Fig. 2A**). Then, the plasma separator was closed to sandwich the whole blood between the two superhydrophobic surfaces. The blood formed a thin film (**Fig. 2B**). The sandwiched blood film was left to sediment for 7-10 min. As seen in the inset of **Fig. 2B**, the blood cells settled towards the bottom of the blood film. After cell sedimentation at room temperature (20-25 °C), the tip of a 200 µL Eppendorf pipette (Brinkman Instruments, Inc., Westbury, NY) was inserted into the plasma exit port to collect plasma (**Fig. 2C**). The plasma containing *S. mansoni* DNA filtered through the Vivid[TM] plasma separation membrane, while the red blood cells (RBCs) and white blood cells (WBCs) were retained in the blood well.

Our separator's recovery efficiency for *S. mansoni* DNA was evaluated against standard laboratory procedures. To establish a reference, anti-coagulated whole blood samples containing *S. mansoni* DNA at various concentrations were centrifuged at a full speed (14,000 rpm) for 10 min using a bench-top centrifuge at room temperature (Labnet International Inc., Woodbridge, NJ). Both *S. mansoni* DNA-laden plasma samples extracted with our plasma separator and separated by the bench-top centrifuge were analyzed by real time LAMP. The *S. mansoni* DNA amount in the plasma samples separated with our device and that of the centrifuged plasma were then compared.
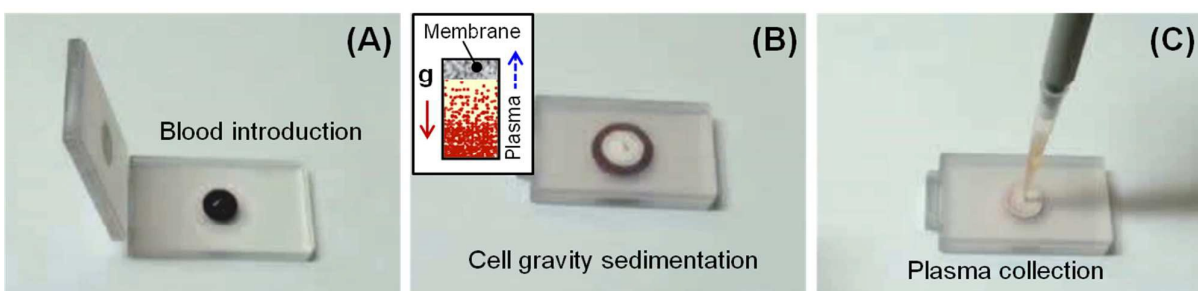

Fig. 2: A sequence of images illustrating the plasma separation process. (A) A 200 µL of blood sample spiked with *S. mansoni* DNA was loaded into the superhydrophobic plasma separator. (B) When the top cover was

closed, the blood was sandwiched between the two superhydrophobic surfaces and formed a thin blood film. After gravitational sedimentation, the top blood layer is much clearer than the bottom layer as schematically shown in the greatly enlarged left inset. (C) A 200 μL pipette was used to collect the plasma through the plasma exit port.

S. mansoni genomic DNA testing

The *S. mansoni* DNA in the separated plasma was subsequently extracted and amplified in our custom-made microfluidic chip.[26,43] Briefly, the chip contains three independent, multifunctional, isothermal amplification reactors. Each of these reactors is equipped with a flow-through Qiagen[TM] silica membrane (QIAamp DNA Blood Mini Kit) at its entry port. The 30 μL of plasma collected with our plasma separator was mixed with 30 μL of Qiagen[TM] lysis buffer and inserted into one of the amplification reactors. The nucleic acids bound to the Qiagen[TM] silica membrane. Subsequent to the sample introduction, 50 μL of Qiagen[TM] wash buffer 1 (AW1) was injected into the chip to remove any remaining amplification inhibitors. Then, the silica membrane was washed with 50 μL of Qiagen[TM] wash buffer 2 (AW2), followed by air-drying for 30 seconds. Next, 22 μL of LAMP master mixture, which contained all the reagents necessary for the LAMP including $0.5 \times$ EvaGreen[@] fluorescence dye (Biotium, Hayward, CA), was injected into each reaction chamber through the inlet port. The target for LAMP amplification was the highly-repetitive Sm1-7 sequence of the *S. mansoni* genomic DNA. The primers were described elsewhere.[44] The molecular diagnostic chip was placed on a homemade, portable heater and heated to 63 ºC for ~ 60 minutes. The fluorescence excitation and emission imaging were carried out with a handheld, USB-based, fluorescence microscope (AM4113T-GFBW Dino-Lite Premier, AnMo Electronics, Taipei, Taiwan).[45]

Results and discussions

Biocompatibility of the spray-on superhydrophobic surface

Inspired by nature, various methods for the preparation of biomimetic superhydrophobic surfaces have been reported,[46] including electrochemical deposition,[47] templating method,[48] self-assembly,[49] and micro-/nanofabrication.[50] Here, we sprayed a superhydrophobic coating on our plasma separator by using a commercially available "Neverwet[TM]." The spray-on "Neverwet[TM]" contains organic

solvent (*i.e.*, acetone, xylene, liquefied petroleum gas) and silica.[51] We selected this particular surface treatment method because of its simplicity, low cost, and compatibility with various materials. **Fig. 3** shows the morphologies of the spray-on superhydrophobic surface and non-coated 3D-printed substrate. The coated surface features micro-/nano- scale asperities (**Fig. 3A**) that render the surface superhydrophobic with a water contact angle of 152° (inset in **Fig. 3A**). In contrast, the uncoated substrate is smooth (**Fig. 3B**) with a contact angle of 71.6° (inset in **Fig. 3B**).
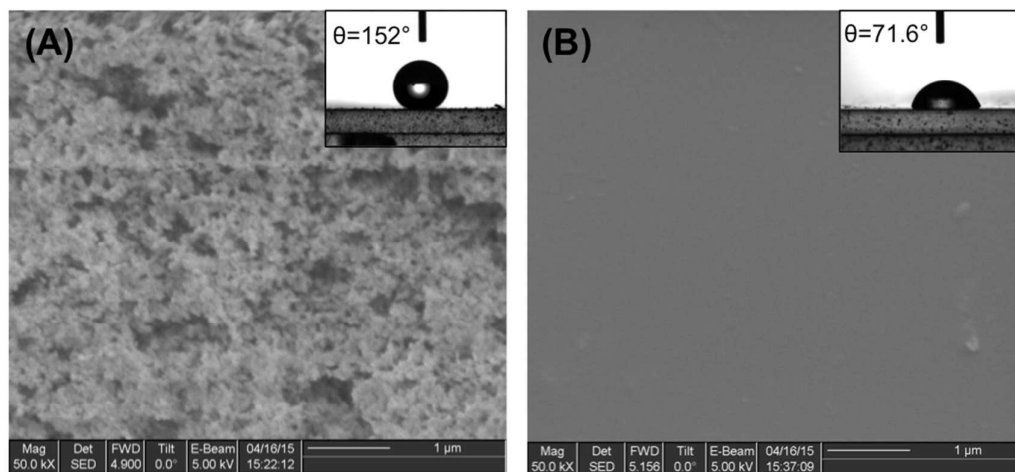

Fig. 3: SEM images of the substrates with (A) and without (B) the spray-on superhydrophobic coating. Inset: static water contact angle of a 5 μL water droplet on the respective surface.

We further evaluated the biocompatibility of the spray-on superhydrophobic coating, with regard to biomolecular adhesion, blood-clotting time, and hemocompatibility. The spray-on superhydrophobic coating had only 2.6% DNA loss, which was 9 times lower than that of the non-coated substrate (23.9%), in the presence of 0.5 pg/mL *S. mansoni* genomic DNA in plasma. This striking reduction in absorption may be attributed to the reduced liquid-solid contact area due to the presence of air pockets entrapped among the micro-/nanoscale hierarchical structures of the superhydrophobic coating.

Hemolysis should be avoided since lysis of red blood cells introduces hemoglobin, a strong inhibitor of both enzymatic amplification and ELISA, into the plasma. In the presence of hemoglobin, there are two absorbance peaks: one at 540 and another at 576 nm. We compared the absorbance spectra of the plasma extracted by our device with the spectra of centrifuged plasma using a

9

benchtop instrument (**Fig. S3** in Supporting Information). There are no obvious absorbance peaks at 540 and 576 nm for both the on-chip separated plasma sample and the benchtop centrifuged plasma. To assess the hemocompatibility of the superhydrophobic coating, we defined the hemolysis rate (HR) as the ratio of the optical density (OD) difference between the test sample (OD_{test}) and the negative control ($OD_{negative}$) *vs.* the OD difference of the positive ($OD_{positive}$) and negative ($OD_{negative}$) controls.[52] Our experiments show that the hemolysis ratio of blood on the spray-on superhydrophobic surface is about one-ninth of that of the uncoated substrate, providing direct evidence of the enhanced hemocompatibility of the superhydrophobic surface.

In addition, we did not observe any blood clotting on the superhydrophobic surface (**Fig. 4A**) after incubation with 30 μL of whole blood at 37 °C for 20 min. In contrast, a large blood clot appeared on the surface of the uncoated substrate (**Fig. 4B**), suggesting that our superhydrophobic surface had good blood compatibility in preventing thrombus formation.
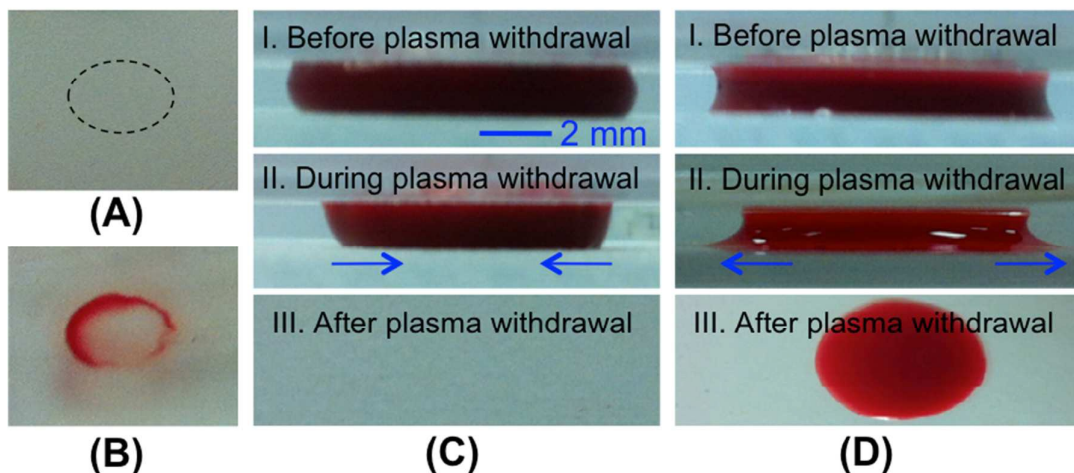

Fig. 4: Photographs of blood clots on the spray-on superhydrophobic substrate (A) and on the uncoated substrate (B) after incubation with whole blood at 37 °C for 20 min. The dashed ellipse indicates the location of the blood drop on the superhydrophobic substrate (A). A sequence of images illustrating the plasma separation from whole blood film sandwiched between two superhydrophobic substrates (C) and uncoated substrates (D).

Top-positioned membrane-based, sedimentation-assisted, separation mechanism

In conventional membrane-based separation,[22-24] the plasma separation membrane is placed horizontally at the bottom of the sample introduction chamber. Since the blood cells are heavier than

the plasma, they sediment directly on the membrane surface. Although this arrangement exposes the membrane to a spatially uniform cell concentration, the membrane is easily blocked by the blood cells. In contrast, here, we propose a top-positioned membrane to facilitate sedimentation-assisted, separation, increase membrane separation capacity, and improve plasma yield. The top-positioned membrane configuration allows for gravitational sedimentation of the blood cells away from the membrane surface (Inset in **Fig. 2B**) rather than precipitation directly onto the membrane surface.[22-24] This arrangement reduces the membrane blockage by blood cells and increases the membrane separation capacity without excessive hemolysis.

In operation, the blood drop is placed in the blood well and a few minutes are allowed for the blood cells to sediment. The gravitational sedimentation process of the blood cells is shown in **Fig. S4** in Supporting Information. After the sedimentation, a pipette is inserted into the plasma exit port at the top cover (**Fig. 2C**). When a negative pressure is applied by the pipette, the resulting pressure difference across the membrane induces plasma flow through the membrane while the blood cells are left behind. Since the pipette provides a continuous negative pressure and the flow velocity of the plasma is low (~60 μL/min), re-floating of blood cells does not occur during plasma extraction. Plasma filtered through the separation membrane enters the space among the micropillars. This space constitutes the dead volume of the device. When selecting the micropillar dimensions, we attempted to minimize the dead volume among the micropillars and the micropillars' surface area while maintaining dimensions compatible with the tolerances of our 3D-printer. The array's pitch was selected small enough to prevent excessive sagging of the membrane during the application of negative back pressure. Since the volume among the micropillars is less than 5% of the volume of the plasma separated in a typical device, reducing the micropillars' heights will complicate the manufacturing process while yielding diminishing gains in performance. Thus, we selected 300 μm tall micropillars as a reasonable compromise.

Figs. 2 and **4C**, and **Video S1** in Supporting Information illustrate in detail the operation of the superhydrophobic plasma separator**.** When blood was sandwiched between two superhydrophobic substrates, a thin, well-defined, blood film with a high contact angle was formed as shown in **Fig. 4C-I**. When the plasma was withdrawn, the sandwiched blood film contracted (indicated by arrows in **Fig. 4C-II**) and no blood was left on the superhydrophobic substrate (**Fig. 4C-III**) after plasma withdrawal. This is in sharp contrast with the performance of the uncoated substrates, on which the

11

blood spread and remained (**Fig. 4D**).

Our superhydrophobic plasma separator with the top-positioned separation membrane extracted 65 ±21.5 μL (n=10) of plasma from 200 μL of undiluted whole blood. This corresponds to a membrane separation capacity of 130 μL/cm^2, which is 6.5 times higher than the value (20 μL/cm^2) specified by the Vivid^{TM} membrane manufacturer.[53]

Next, we compare the plasma volume (V_{device}) separated with our device with the plasma volume ($V_{centrifugation}$) separated with a benchtop centrifugation method. We define our device's yield Y= V_{device}/ $V_{centrifugation}$ × 100%. We find, Y=70± 23% (n=10). Although we designed our device to extract plasma from 200 μL of whole blood (which is comparable to the volume extracted from a finger-prick, i.e., 250-500 μL[32,33]), our plasma separator can be tailored to operate with other volumes of whole blood with only slight design modifications. As seen in **Fig. S5** in Supporting Information, by increasing the size of the separation membrane and the blood well, we separated plasma from 800 μL of whole blood.

S. mansoni genomic DNA detection on a molecular diagnostic chip

Schistosomiasis is the second most prevalent parasitic disease in the tropics and subtropics.[54,55] About 779 million people in 77 endemic countries live in areas where the risk of infection is high. Since our main objective in separating the plasma from the whole blood is to detect cell-free DNA and plasma pathogens by molecular diagnostics, it is necessary to know whether our separation process affects the *S. mansoni* genomic DNA concentration in the plasma. Loss of targets can occur, for example, due to non-specific binding of the DNA to the separation membrane and the various structural constituents of the separator, *e.g.* the micropillar array with its relatively high surface area. To test the DNA recovery, we constructed a 3D-printed tube (**Fig. S6** in Supporting Information) with a 1.5 mm diameter Qiagen^{TM} silica membrane to extract *S. mansoni* genomic DNA from 30 μL of plasma separated with our plasma separator. The extracted DNA was quantified by real time LAMP method on a benchtop PCR machine. The on-chip extracted plasma showed a *S. mansoni* genomic DNA recovery yield of > 84.5 ± 25.8 % (n=3) (**Fig. 5A)** when compared with traditional centrifugation method. As the *S. mansoni* genomic DNA in the whole blood increased, so did the recovery rate. This increase in recovery rate could be due to the saturation of non-specific surface binding sites in the device. These results clearly demonstrate that our superhydrophobic plasma separation device with a top-positioned membrane has a great potential for use in clinical, molecular

testing with downstream detection assays with minimal loss of target biomolecules.

To test the suitability of the plasma extracted with our separator for point-of-care, nucleic acid-based detection, we separated plasma from schistosome DNA-spiked blood using our superhydrophobic separation device, and then carried out the amplification process in our molecular diagnostic chip.[26] **Fig. 5B** depicts fluorescence emission of intercalating fluorescent dye in three amplification chambers of our molecular diagnostic chip at the end of LAMP amplification of plasma samples spiked with different concentration of *S. mansoni* genomic DNA. The target *S. mansoni* genomic DNA amount in each chamber was 10 fg, 1 fg and 0 fg (negative control) (left to right). The test reaction chambers with positive samples emitted a strong green fluorescence due to the amplification of target DNA molecules while the negative control chamber did not show any emission. Our molecular diagnostic chip was able to detect as few as 0.5 fg of *S. mansoni* genomic DNA (based on the *S. mansoni* genome size of ~365 Mb[56], a single genome equivalent is 0.4 pg). This experiment indicates that the plasma separated by our superhydrophobic plasma separator is suitable for nucleic acid amplification.
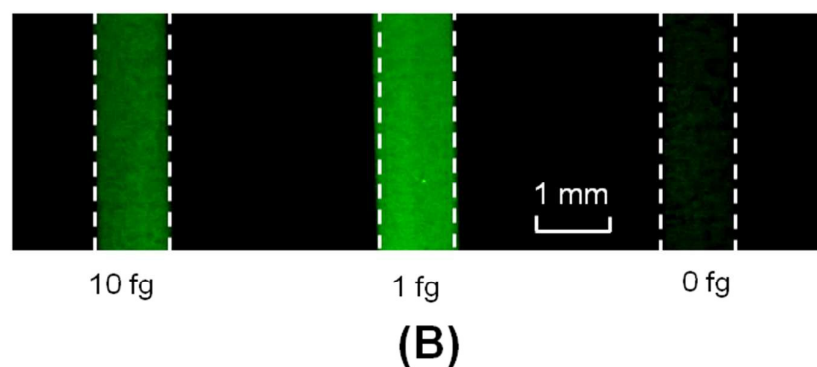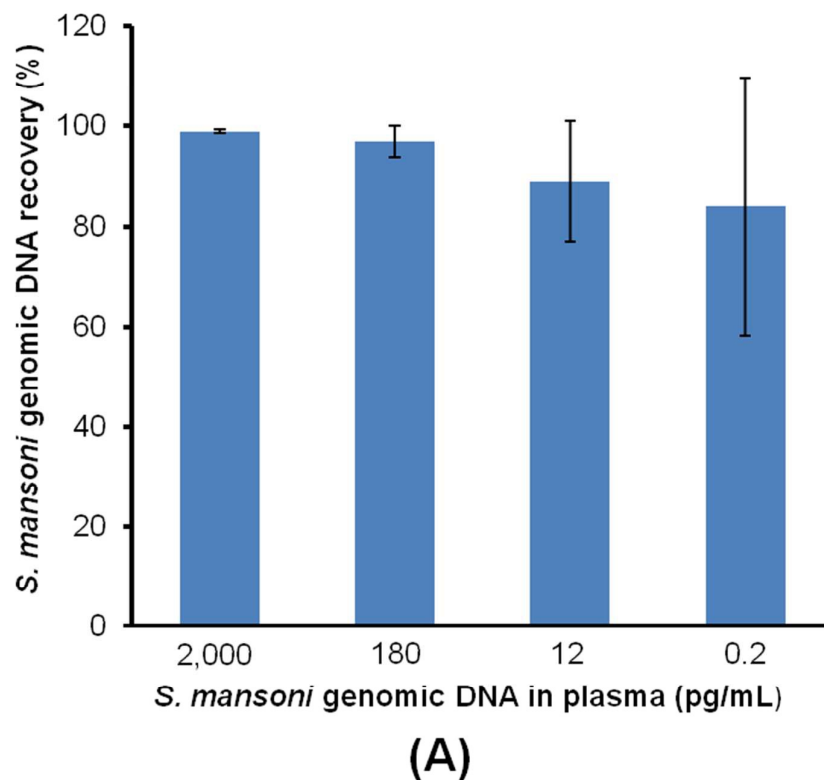
Fig. 5: (A) Recovery efficiency of *S. mansoni* genomic DNA on our plasma separator at various concentrations. (B) Endpoint, fluorescence images of intercalating dye in three amplification chambers, target DNA amount in each chamber is 10 fg, 1 fg and 0 fg (negative control) (left to right). The dashed squares outline the locations of the amplification reactors.

Conclusions and outlook

We described a simple, high-efficiency, clamshell-style, superhydrophobic plasma separator for the extraction of plasma from whole blood. Our separator takes advantage of de-wetting phenomena and biocompatibility of superhydrophobic surfaces. Unique to our device is the combined use of multiple

separation principles and strategies, including cell sedimentation, size-based filtration, and lotus-leaf effect. The top-positioned, membrane-based, separation mechanism improves performance with respect to sample volume capacity and plasma yield, while the superhydrophobic surfaces offer minimal hemolysis or contamination of the plasma with substances such as hemoglobin, and reduce losses of the target analytes (*i.e*. DNA) due to unwanted surface binding. The plasma yield of our device is about 70% of centrifugation-based benchtop processes.

We have demonstrated that the plasma extracted with our plasma separator is appropriate for molecular detection of target analytes contained in whole blood by spiking blood with *S. mansoni* genomic DNA and using the plasma in the microfluidic-based nucleic acid amplification. We demonstrated a high efficiency recovery of nucleic acids (> 84.5 ± 25.8 %).

Most of our experiments focused on blood volumes that can be obtained from a finger prick and we demonstrated the separation of 65±21.5 µL of plasma from 200 µL of whole blood. By simple design changes, our device can be adapted to operate with other whole blood volumes. We fabricated our prototypes using 3D-printing. The use of 3D printer is ideal for device design as it allows a rapid turn around between design and prototype. This manufacturing method is too slow, however, for mass production. For mass production, our separator will likely need to be manufactured by injection molding.

The superhydrophobic, easy-to-use plasma separator reported herein can be used as a stand-alone separation device at home, in the clinic, as well as in resource-constrained settings where funds and trained personnel are in short supply. Moreover, the simplicity of the format, non-instrumented operation and the ability to integrate with existing microfluidic devices will provide for convenient uses in downstream processing and analysis.[57]

Acknowledgments

References

1 W. A. Al-Soud, P. Rådström, *J Clin Microbiol*, 2001, **39**, 485-493.

15

2   T. Raivio, I. R. Korponay-Szabó, T. Paajanen, M. Ashorn, S. Iltanen, P. Collin, K. Laurila, E. Nemes, J. B. Kovács, G. Carrard, M. Saramäki, M. Mäki, K. Kaukinen, *J Pediatr Gastroenterol Nutr*, 2008, **47**, 562-567.

3   P. L. Corstjens, L. van Lieshout, M. Zuiderwijk, D. Kornelis, H. J. Tanke, A. M. Deelder, G. J. van Dam, *J Clin Microbiol*, 2008, **46**, 171-176.

4   C. Drosten, M. Panning, J. F. Drexler, F. Hänsel, C. Pedroso, J. Yeats, L. K. de Souza Luna, M. Samuel, B. Liedigk, U. Lippert, M. Stürmer, H. W. Doerr, C. Brites, W. Preiser, *Clin Chem*, 2006, **52**, 1258-1266.

5   M. Giordano, T. Kelleher, R. J. Colonno, A. Lazzarin, K. Squires, *J Clin Virol*, 2006, **35**, 420-425.

6   I. Sbarsi, P. Isernia, L. Montanari, C. Badulli, M. Martinetti, L. Salvaneschi, *Blood Transfus*, 2012, **10**, 34-38.

7   A. Nabatiyan, Z. A. Parpia, R. Elghanian, D. M. Kelso, *J. Virol Methods*, 2011, **173**, 37-42.

8   K. K. Lee, C. H. Ahn, *Lab Chip*, 2013, **13**, 3261-3267.

9   I. K. Dimov, L. Basabe-Desmonts, J. L. Garcia-Cordero, B. M. Ross, Y. Park, A. J. Ricco, L. P. Lee, *Lab Chip*, 2011, **11**, 845-850.

10 J. H. Son, S. H. Lee, S. Hong, S. M. Park, J. Lee, A. M. Dickey, L. P. Lee, *Lab Chip*, 2014, **14**, 2287-2292.

11 V. VanDelinder, A. Groisman, *Anal. Chem*, 2006, **78**, 3765-3771.

12 T. Tachi, N. Kaji, M. Tokeshi, Y. Baba, *Anal Chem*, 2009, **81**, 3194-3198.

13 D. J. Brambilla, C. Jennings, R. Morack, S. Granger, J. W. Bremer, *J. Clin. Microbiol*, 2004, **42**, 2819-2820.

14 G. G. Sherman, G. Stevens, S. A. Jones, P. Horsfield, W. S. Stevens, *J Acquir Immune Defic Syndr*, 2005, **38**, 615-617.

15 N. Mehta, S. Trzmielina, B. A. Nonyane, M. N. Eliot, R. Lin, A. S. Foulkes, K. McNeal, A. Ammann, V. Eulalievyolo, J. L. Sullivan, K. Luzuriaga, M. Somasundaran, *PLoS One*, 2009, **4**, e5819.

16 A. K. Pathak, M. Bhutani, S. Kumar, A. Mohan, R. Guleria, *Clin Chem*, 2006, **52**, 1833-1842.

17 H. Schwarzenbach, D. S. Hoon, K. Pantel, *Nat Rev Cancer*, 2011, **11**, 426-437.

18 M. Tsujiura, D. Ichikawa, S. Komatsu, A. Shiozaki, H. Takeshita, T. Kosuga, H. Konishi, R.

Morimura, K. Deguchi, H. Fujiwara, K. Okamoto, E. Otsuji, *Br J Cancer*, 2010, **102**, 1174-1179.

19   M. Urbanova, J. Plzak, H. Strnad, J. Betka, *Cell Mol Biol Lett*, 2010, **15**, 242-259.

20   D. C. García-Olmo, C. Domínguez, M. García-Arranz, P. Anker, M. Stroun, J. M. García-Verdugo, D. García-Olmo, *Cancer Res*, 2010, **70**, 560-567.

21   WHO online. http://www.who.int/hiv/pub/guidelines/arv2013/art/artmonitoring/en/index4.html (accessed September 2015)

22   A. Homsy, P. D. van der Wal, W. Doll, R. Schaller, S. Korsatko, M. Ratzer, M. Ellmerer, T. R. Pieber, A. Nicol, N. F. de Rooij, *Biomicrofluidics*, 2012, **6**, 12804−128049.

23   S. Wang, D. Sarenac, M. H. Chen, S. H. Huang, F. F. Giguel, D. R. Kuritzkes, U. Demirci, *Int. J. Nanomedicine*, 2012, **7**, 5019−5028.

24   M. M. Gong, B. D. Macdonald, T. Vu Nguyen, K. Van Nguyen, D. Sinton, *Biomicrofluidics*, 2013, **7**, 44111.

25   A. Nabatiyan, Z. A. Parpia, R. Elghanian, D. M. Kelso, *J Virol Methods*, 2011, **173**, 37-42.

26   C. Liu, M. Mauk, R. Gross, F. D. Bushman, P. H. Edelstein, R. G. Collman, H. H. Bau, *Anal Chem*, 2013, **85**, 10463-10470.

27   E. Vardas, M. Mathai, D. Blaauw, J. McAnerney, A. Coppin, J. Sim, *J Med Virol*, 1999, **58**, 111-115.

28   J. Pavie, A. Rachline, B. Loze, L. Niedbalski, C. Delaugerre, E. Laforgerie, J. C. Plantier, W. Rozenbaum, S. Chevret, J. M. Molina, F. Simon, *PLoS One*, 2010, **5**, e11581.

29   J. C. Patton, E. Akkers, A. H. Coovadia, T. M. Meyers, W. S. Stevens, G. G. Sherman, *Clin Vaccine Immunol*, 2007, **14**, 201-203.

30   D. K. Glencross, L. M. Coetzee, M. Faal, M. Masango, W. S. Stevens, W. F. Venter, R. Osih, *J Int AIDS Soc*, 2012, **15**, 3.

31   V. Jain, T. Liegler, J. Kabami, G. Chamie, T. D. Clark, D. Black, E. H. Geng, D. Kwarisiima, J. K. Wong, M. Abdel-Mohsen, N. Sonawane, F. T. Aweeka, H. Thirumurthy, M. L. Petersen, E. D. Charlebois, M. R. Kamya, D. V. Havlir, SEARCH Collaboration, *Clin Infect Dis*, 2013, **56**, 598-605.

32   J. H. Kattenberg, C. M. Tahita, I. A. Versteeg, H. Tinto, M. Traoré‐Coulibaly, H. D. Schallig, P. F. Mens, *Tropical Medicine & International Health*, 2012, **17**, 550-557.

33   F. O. ter Kuile, D. J. Terlouw, S. K. Kariuki, P. A. Phillips-Howard, L. B. Mirel, W. A. Hawley,

J. F. Friedman, Y. P. Shi, M. S. Kolczak, A. A. Lal, J. M. Vulule, B. L. Nahlen, *Am J Trop Med Hyg.* 2003, **68**, 68-77.

34   J. Zhao, L. Song, J. Yin, W. Ming, *Chem Commun (Camb)*, 2013, **49**, 9191-9193.

35   M. Jönsson-Niedziółka, F. Lapierre, Y. Coffinier, S. J. Parry, F. Zoueshtiagh, T. Foat, V. Thomy, R. Boukherroub, *Lab Chip*, 2011, **11**, 490-496.

36   X. Zhang, L. Wang, E. Levänena, *RSC Adv*, 2013, **3**, 12003-12020.

37   X. Hou, X. Wang, Q. Zhu, J. Bao, C. Mao, L. Jiang, J. Shen, *Colloids Surf B Biointerfaces*, 2010, **80**, 247-250.

38   F. Mumm, A. T. van Helvoort, P. Sikorski, *ACS Nano*, 2009, **3**, 2647-2652.

39   S. Xing, R. S. Harake, T. Pan, *Lab on Chip*, 2011, **11**, 3642-3648

40   C. Liu, *Microfluidics and Nanofluidics*, 2010, **9**, 923-931.

41   J. Y. Shiu, P. L. Chen, *Advanced Functional Materials*, 2007, **17**, 2680-2686.

42   Rust-Oleum   online. http://www.rustoleum.com/product-catalog/consumer-brands/neverwet/neverwet-kit/   (accessed November 2015)

43   C. Liu, E. Geva, M. Mauk, X. Qiu, W. R. Abrams, D. Malamud, K. Curtis, S. M. Owen, H. H. Bau, *Analyst*, 2011, **136**, 2069-2076.

44   I. Abbasi, C. H. King, E. M. Muchiri, J. Hamburger, *Am J Trop Med Hyg.*, 2010, 83(2):427-32.

45   C. Liu, M. M. Sadik, M. G. Mauk, P. H. Edelstein, F. D. Bushman, R. Gross, H. H. Bau, *Sci Rep*, 2014, **4**, 7335.

46   S. S. Latthe, A. B. Gurav, C. S. Maruti, R. S. Vhatkar, *Journal of Surface Engineered Materials and Advanced Technology*, 2012, **2**, 76-94.

47   M. Li, J. Zhai, H. Liu, Y. Song, L. Jiang, D. Zhu, *J. Phys. Chem. B*, 2003, **107**, 9954-9957.

48   M. Jin, X. Feng, L. Feng, T. Sun, J. Zhai, T. Li, L. Jiang, *Advanced Materials*, 2005, **17**, 1977-1981.

49   Y. Rahmawan, L. Xua; S. Yang, *J. Mater. Chem. A*, 2013, **1**, 2955-2969.

50   X. Zhang, Q. Di, F. Zhu, G. Sun, H. J. Zhang, *Nanosci. Nanotechnol*, 2013, **13**, 1539-1542.

51   http://www.rustoleumspraypaint.com/product/neverwet-2/ (accessed November 2015)

52   Y. Yang, Y. Lai, Q. Zhang, K. Wu, L. Zhang, C. Lin, P. Tang, *Colloids Surf B Biointerfaces*, 2010, **79**, 309-313.

53 Pall Life Sciences online.

https://www.pall.com/pdfs/OEM-Materials-and-Devices/09.2730_VividPlasma_DS_6pg.pdf

(accessed November 2015)

54 A. C. Clements, A. Garba, M. Sacko, S. Touré, R. Dembelé, A. Landouré, E. Bosque-Oliva, A. F. Gabrielli, A. Fenwick, *Emerg Infect Dis*, 2008, **14**, 1629-1632.

55 C. F. Hatz, *J Travel Med*, 2005, **12**, 1-2.

56 A. V. Protasio, I. J. Tsai, A. Babbage, S. Nichol, M. Hunt, M. A. Aslett, N. De Silva, G. S. Velarde, T. J. Anderson, R. C. Clark, C. Davidson, G. P. Dillon, N. E. Holroyd, P. T. LoVerde, C. Lloyd, J. McQuillan, G. Oliveira, T. D. Otto, S. J. Parker-Manuel, M. A. Quail, R. A. Wilson, A. Zerlotini, D. W. Dunne and M. Berriman, *PLoS Neglected Tropical Diseases*, 2012, **6**, e1455.

57 D. Chen, M. Mauk, X. Qiu, C. Liu, J. Kim, S. Ramprasad, S. Ongagna, W. R. Abrams, D. Malamud, P. L. Corstjens, H. H. Bau, *Biomed Microdevices*, 2010, **12**, 705-719.